

MECHANICAL STRENGTH AND FRACTURE OF Sigma 1140+ SiC FIBRES

C. González and J. LLorca

Department of Materials Science, Polytechnic University of Madrid
E. T. S. de Ingenieros de Caminos, 28040 – Madrid, Spain

ABSTRACT

Tensile tests were carried out in pristine Sigma 1140+ SiC fibres and in fibres extracted from a Ti-6Al-4V-matrix composite. The elastic modulus and the tensile strength were computed after measuring carefully the fibre diameter. The average fibre strength was reduced by 20% and the Weibull modulus by half during composite processing. The analysis of the fracture surfaces in the scanning electron microscope showed that the strength-limiting defects were located around the tungsten core in pristine fibres and at the surface in fibres extracted from the composite panels. These latter defects were nucleated by the mechanical stresses generated on the fibres during the panel consolidation.

INTRODUCTION

In the present state of technological development, ceramic fibres stand among the stiffest and strongest materials. Fibre stiffness comes from their strong covalent or ionic bond, while strength is dictated by the longest defect, whose size can be reduced to very small values through the appropriate processing techniques. Nevertheless, ceramic fibres are brittle and have to be used embedded in a matrix, which maintains the fibers oriented in the optimum direction, distributes the concentrated loads, and protects the fibers against wear and chemical attack from the environment. Fibre handling and fibre/matrix interfacial reactions during composite processing may nucleate defects on the fibre surface, which will reduce the fibre properties as well as those of the composite. This phenomenon is analysed in this paper in a Ti-6Al-4V composite reinforced with Sigma 1140+ SiC fibres. To this end, the Weibull parameters for the fibre strength were measured on as-fabricated fibres and on fibres extracted from the composite, and the differences between them were explained through fractographic observations in the scanning electron microscope.

MATERIALS AND EXPERIMENTAL TECHNIQUES

Composite panels of a Ti-6Al-4V matrix uniaxially reinforced with 35 vol. % Sigma 1140+ monofilaments were manufactured by DERA (United Kingdom) through conventional foil-fibre-foil processing. The panels of 1.35 mm in thickness were consolidated in vacuum at 940 °C during 1 hour under 30 MPa of pressure. The matrix filled completely the spaces between the fibres and no porosity was detected in the composite. The cross-section of a Sigma 1140+ fibre within the matrix is shown in Figure 1. The fibres were processed by chemical vapour deposition of β -SiC from a mixture of dichloromethylsilane and hydrogen on a 15 μ m diameter tungsten wire. A carbon coating was finally deposited in a separate reactor from a mixture of propane and chloroform in argon. More details of the fibre microstructure can be found elsewhere [1].

Two groups of fibres were tested. The first were extracted from the composite by removing the matrix with an aqueous solution of HF acid at 40%. The second were provided by the manufacturer in the as-fabricated condition. Some as-fabricated fibres were placed in the HF solution and tested afterwards to ascertain the effect

of the acid on the fibre properties.

Fibre strength was determined through tensile tests. The fiber ends were glued with cyanoacrylate on cardboards, which were connected by mechanical grips to an Instron 4505 mechanical testing machine. Tests were carried out under stroke control at a cross-head speed of 50 μm per minute, and the maximum load was measured with a 100 N load cell. Fibres were handled with extreme care to avoid damage to the fibre surface. This experimental set-up was also used to measure the elastic modulus of the extracted fibres. Two cardboard flags were glued with cyanocrylate along the fibre to measure its deformation with a laser extensometer (Zygo 2100). The initial separation between the flags (around 30 mm) was selected to ensure enough precision in the determination of the longitudinal strain. The distance between the flags and the applied load were continuously monitored during the tensile tests from the readings of the laser extensometer and of the load cell.

The diameter of the various regions in the fibre was measured in an optical microscope. The as-fabricated fibres were carefully aligned and embedded in an epoxy matrix to produce an epoxy-matrix composite. Sections transversal to the fibres were cut from the epoxy- and Ti-matrix composites, and polished on SiC paper to 500 grit finish. This was followed by polishing on a diamond slurry (up to 1 μm) and finally on magnesia. In addition, the fracture surface of the fibres broken in the tests were recovered in some cases and examined in a Jeol 6300 scanning electron microscope to ascertain the characteristics of the critical defects which led to the fibre failure.

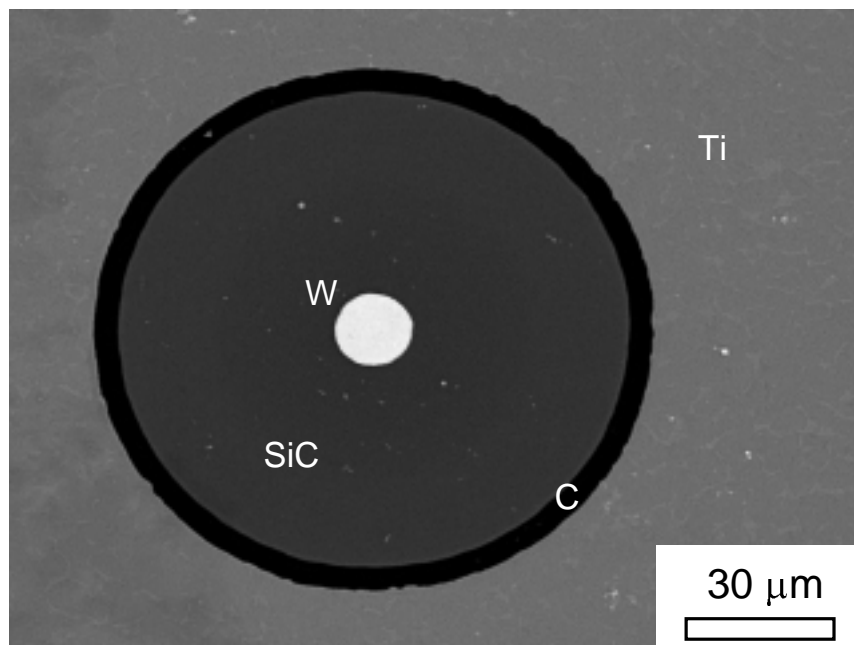


Figure 1: Back-scattered electron micrograph of a Sigma 1140+ monofilament cross-section embedded in the Ti-6Al-4V matrix. The tungsten core, SiC central region, and C coating are easily distinguished.

FIBRE CROSS-SECTION

The fibre diameter, the tungsten core diameter and the thickness of the C sheath were determined through quantitative microscopy. The quantitative analysis included 8 as-fabricated and 42 as-extracted fibres, and the average values are shown in Table 1 together with the corresponding standard deviations. The fibre cross-section was circular (the differences in the length of perpendicular diameters were always below 1%), and all the fibre diameters were between 103 μm and 105 μm for the as-fabricated fibres and between 105 μm and 108 μm for the as-extracted ones.

TABLE 1
DIMENSIONS OF THE SIGMA 1140+ FIBRE FEATURES

	W core	C sheath	Fibre diameter
As-fabricated	$14.8 \pm 0.5 \mu\text{m}$	$4.3 \pm 0.3 \mu\text{m}$	$104 \pm 0.9 \mu\text{m}$
As-extracted	$15.0 \pm 0.3 \mu\text{m}$	$4.4 \pm 0.2 \mu\text{m}$	$107 \pm 0.9 \mu\text{m}$

ELASTIC MODULUS

Cardboard flags were glued to six as-fabricated fibres, which were loaded up to an approximate stress of 2 GPa and unloaded. This process was repeated several times in each fibre, and the load and the displacement between the flags were recorded in a computer. All the fibres exhibited a linear elastic behaviour, and the loading-unloading curves did not present any hysteresis. After the test, the fibres were embedded in epoxy resin to measure the fibre diameter as indicated above, and the average fibre diameter in Table 1 was used to compute the stress-strain curves, which are shown in Figure 2.

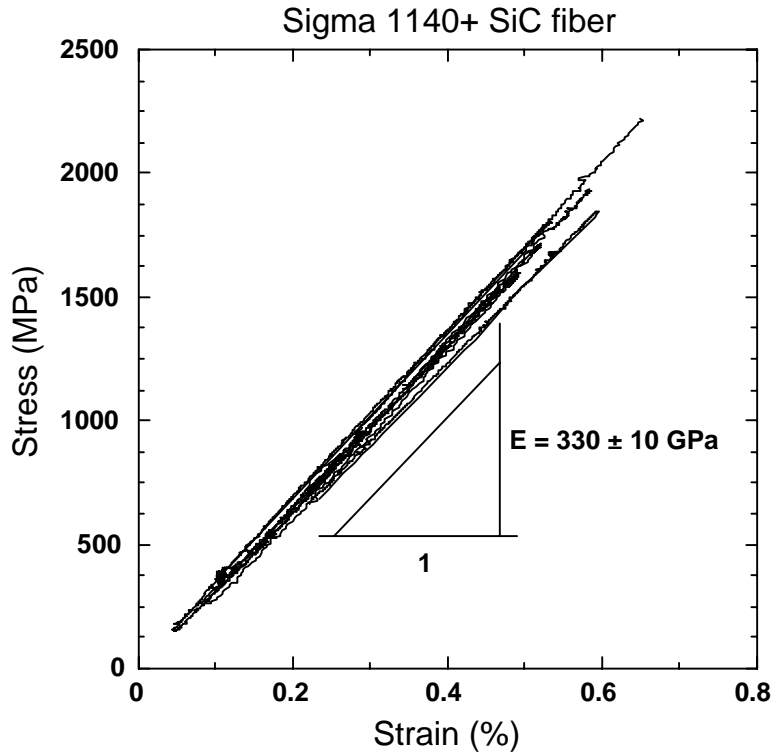


Figure 2: Loading-unloading stress-strain curves for six as-fabricated Sigma 1140+ fibres.

The longitudinal elastic modulus was determined from the slope of the curves in Figure 2, as 330 ± 10 GPa. It is interesting to compare this value with the results of a simple isostrain model, which gives the following expression for the modulus,

$$E = \frac{E_{SiC}\Omega_{SiC} + E_W\Omega_W + E_C\Omega_C}{\Omega} \quad (1)$$

where Ω , Ω_{SiC} , Ω_W , and Ω_C stand respectively for the cross-sections of the fibre and of the three phases within the fibre. Literature data give $E_W = 350$ GPa and $E_{SiC} = 430$ GPa for the moduli of tungsten fibre and of β -SiC, [2] while Shatwell [3] measured $E_C = 80$ GPa in these fibres through a bend resonance method. These values give a theoretical value for the fibre elastic modulus of 373 GPa, which is slightly higher than the experimental result.

It should be noted that the contributions of the tungsten core and of the C sheath to the overall fibre stiffness are almost negligible (≈ 7 and 13 GPa for the W and C respectively), and the discrepancy has to be attributed to the actual value of the CVD SiC modulus, which should be around 380 GPa to fit the experimental data. Chen *et al.* [1] detected small grains of free Si in the fibre through X-ray diffraction, and this excess of Si may be partially responsible for this slight reduction in the modulus of the SiC.

FIBRE STRENGTH

The strength of each fibre was computed as the quotient of the fracture load divided by the average fibre cross-section given in Table 1. This method –as opposed to measuring the actual cross-section of each fibre– was supported by the results of a recent round robin carried out under the auspices of the ASTM C28.07.07 task group on Ceramic Fibers [4], and it seems especially appropriate for these fibres, which show very few changes in the diameter as a result of the processing technique. Fifty as-fabricated and fifty as-extracted fibres were tested with 25.4 mm free length between the cardboard supports. In addition, another batch of fifty as-extracted fibres was tested with only 12.7 mm between the cardboard supports. The strength data of each group of tests were arranged in ascending order and a failure probability of $(i-0.5)/N$, was assigned to each strength based on rank statistics, where i is the rank and N is the total number of experimental data.

According to the Weibull analysis, the cumulative fibre fracture probability, F , is given by

$$F = 1 - \exp \left[- \frac{L}{L_0} \left(\frac{\sigma}{\sigma_0} \right)^m \right] \quad (2)$$

where L is the fibre length, L_0 an arbitrary reference length introduced for dimensional purposes, which was taken as equal to 25.4 mm in the present case, and σ_0 and m stand, respectively, for the characteristic strength and the Weibull modulus of the fibre. They can be obtained through the least squares fitting of the experimental results for the fibre cumulative fracture probability (Figure 3), and the corresponding values are shown in Table 2, together with average strength, σ_m . The Weibull parameters for the as-fabricated fibres were equivalent to those reported in previous investigations [5,6]. In addition, it should be noted that the mechanical properties of the as-fabricated fibres which were immersed in the HF solution prior to testing did not show any difference.

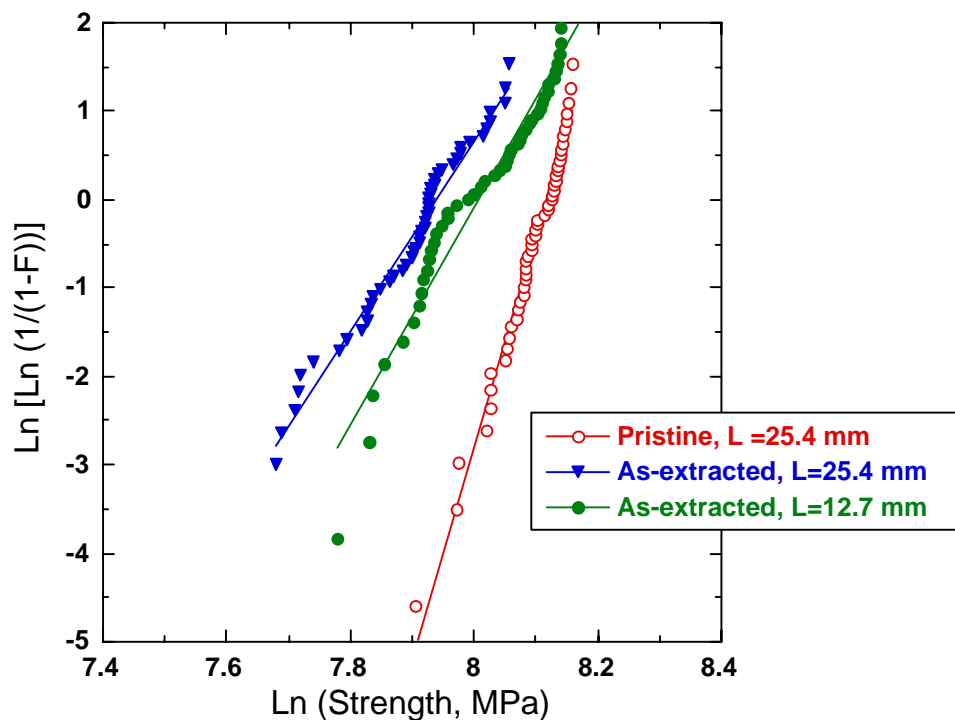


Figure 3: Weibull plot for the strength of as-fabricated and as-extracted Sigma 1140+ SiC fibres.

The application of the Weibull model to ceramic fibres assumes that their strength is controlled by the presence of a population of flaws, homogeneously distributed along the fibre. As a result, the fibre failure probability increases and the fibre characteristic strength decreases with the fibre length (see Table 2). According to eqn (2), σ_0 should be inversely proportional to $L^{1/m}$, and the experimental results for as-extracted fibres of 12.7 mm and 25.4 mm uphold this hypothesis.

TABLE 2
WEIBULL PARAMETERS AND AVERAGE STRENGTH FOR THE SIGMA 1140+ FIBRE

	σ_0 (GPa)	m	σ_m (GPa)
As-fabricated, L=25.4 mm	3.35	23.7	3.27
As- extracted, L=25.4 mm	2.81	10.8	2.68
As- extracted, L=12.7 mm	3.00	12.1	2.88

FRACTOGRAPHY AND DISCUSSION

The fracture surface of the as-fabricated fibres corroborated the results of previous investigations [5,7]: the critical flaws which limited the strength of these fibres were located at the W/SiC interface (Figure 4). The fibres extracted from the composite which presented very high strength also failed by the nucleation of a defect from the core (Figure 5a). The as-extracted fibres with low strength exhibited, however, surface defects, which were responsible for the degradation of the fibre strength and Weibull modulus. This change from fracture nucleated in one type to two types of defects can also be observed in Figure 3. The experimental data for the failure probability of the as-fabricated fibres follow very closely the straight line predicted by the Weibull model, while those measured the as-extracted fibres present much higher dispersion. This indicates that defects of diverse nature and origin were limiting the fibre strength.

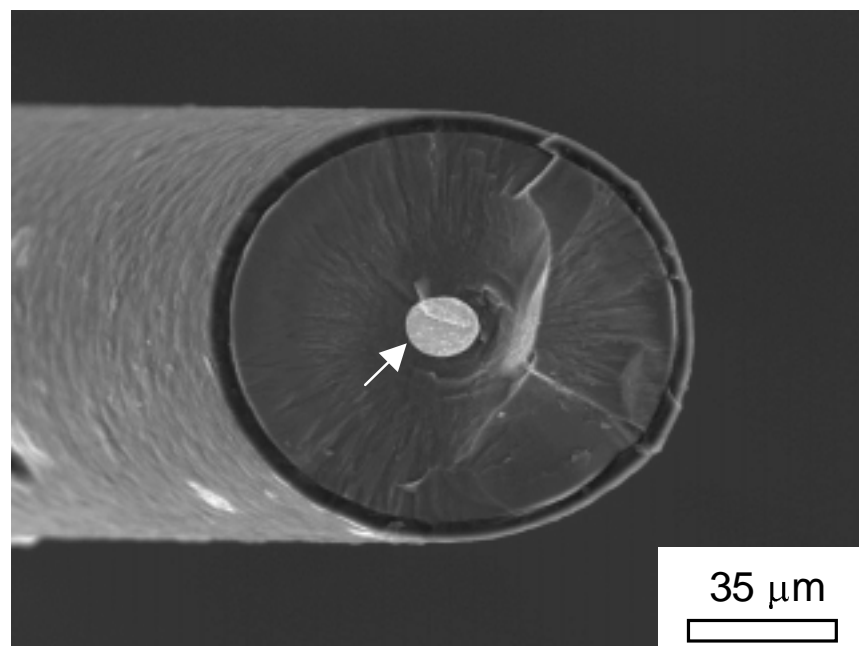


Figure 4: Fracture surface of an as-fabricated fibre broken at 3.27 GPa. Failure was initiated at the W/SiC interface, as shown by the arrow.

The results in Figure 3 also showed that the maximum strength of the as-extracted fibres (3.16 GPa) was significantly lower than that of the as-fabricated ones (3.50 GPa). As the latter fail by defects nucleated at the

W/SiC interface, it could be asked whether an increase in the thickness of the reaction layer at this interface during processing might be responsible for this behaviour. However, Heath [8] did not find any degradation in the strength of C-coated Sigma 1240 fibres treated in nitrogen at 1000°C during 1 hour. His conclusions were supported by the results of reaction kinetics studies, which indicated that several hundreds of hours were necessary to grow a reaction zone of $\approx 0.5 \mu\text{m}$ at the W/SiC interface at temperatures below 950°C. In agreement with these reports, our analyses of the fibre cross-section in the scanning electron microscope did not reveal any differences at the W/SiC interface between as-extracted and as-fabricated fibres, so the strength degradation cannot be attributed to this mechanism.

Baker *et al.* [6] also studied the effect of processing on the strength of Sigma 1140+ fibres of 25.4 mm in length extracted from Ti-6Al-4V-matrix composite panels processed by vacuum plasma spraying followed by consolidation through vacuum hot pressing. The results for panels consolidated at two different temperatures (870 and 920 °C) during approximately 75 minutes are presented in Table 3, together with those for the as-fabricated fibres. The fibres suffered a marked reduction in strength and in the Weibull modulus during processing, which was caused by the nucleation of defects on the fibre surface during consolidation by hot-press, the last step of processing. Fibre damage decreased sharply as the consolidation temperature increased, and this observation excludes a mechanism of strength degradation controlled by the growth of the reaction zone at the W/SiC interface

TABLE 3
WEIBULL PARAMETERS AND AVERAGE STRENGTH FOR THE SIGMA 1140+ FIBRE [6]

	σ_0 (GPa)	m	σ_m (GPa)
As-fabricated	3.14	25	3.07
As-extracted (HP at 870°C)	2.60	4	2.36
As-extracted (HP at 920°C)	2.89	9	2.74

Fibre degradation during processing seems to be induced by the nucleation of flaws at the fibre surface, and it is important to ascertain whether the defects were induced by chemical and/or mechanical factors. A homogeneous reaction layer (thickness under $0.5 \mu\text{m}$) was observed between the C coating and the Ti-matrix in the scanning electron microscope, but this layer was too thin to induce any damage on the fibre. In addition, the C sheath around the fibre was continuous, and regions denuded of this protective layer which may have led to direct contact between Ti and SiC were not detected. Moreover, the surface defects which led to the fibre failure did not present any evidence of chemical species produced by the reaction between Ti and SiC. These observations point to the impingement of matrix asperities through the fibre coating into the underlying SiC as the main cause of fibre damage during processing. This is supported by the work of Baker *et al.* [6], which only found fibre degradation after hot pressing. Neither fibre winding, nor vacuum plasma spraying, nor pressureless consolidation at high temperature reduced significantly the fibre strength.

CONCLUSIONS

The elastic modulus and the tensile strength were measured in pristine Sigma 1140+ SiC fibres and in fibres extracted from a Ti-6Al-4V-matrix composite processed by the foil-fibre-foil method. The fibre elastic modulus (330 ± 10 GPa) was significantly below the theoretical value given by the rule of mixtures (373 GPa) and this may be attributed to the presence of free Si in the fibre [1], which reduces the SiC modulus.

The fibres suffered damage during processing, which resulted in a 20% reduction in the average strength, while the Weibull modulus dropped from ≈ 24 to 11-12. While the as-fabricated fibres failed from cracks nucleated at the inner W/SiC interface, fracture of as-extracted fibres was initiated at the fibre surface. These defects were very likely caused by the impingement of matrix asperities through the fibre coating into the underlying SiC during composite consolidation at high temperature and pressure. As the overall composite performance depends on the fibre strength, it is important to devise improved coatings and to optimise the processing parameters in

order to minimise fibre damage

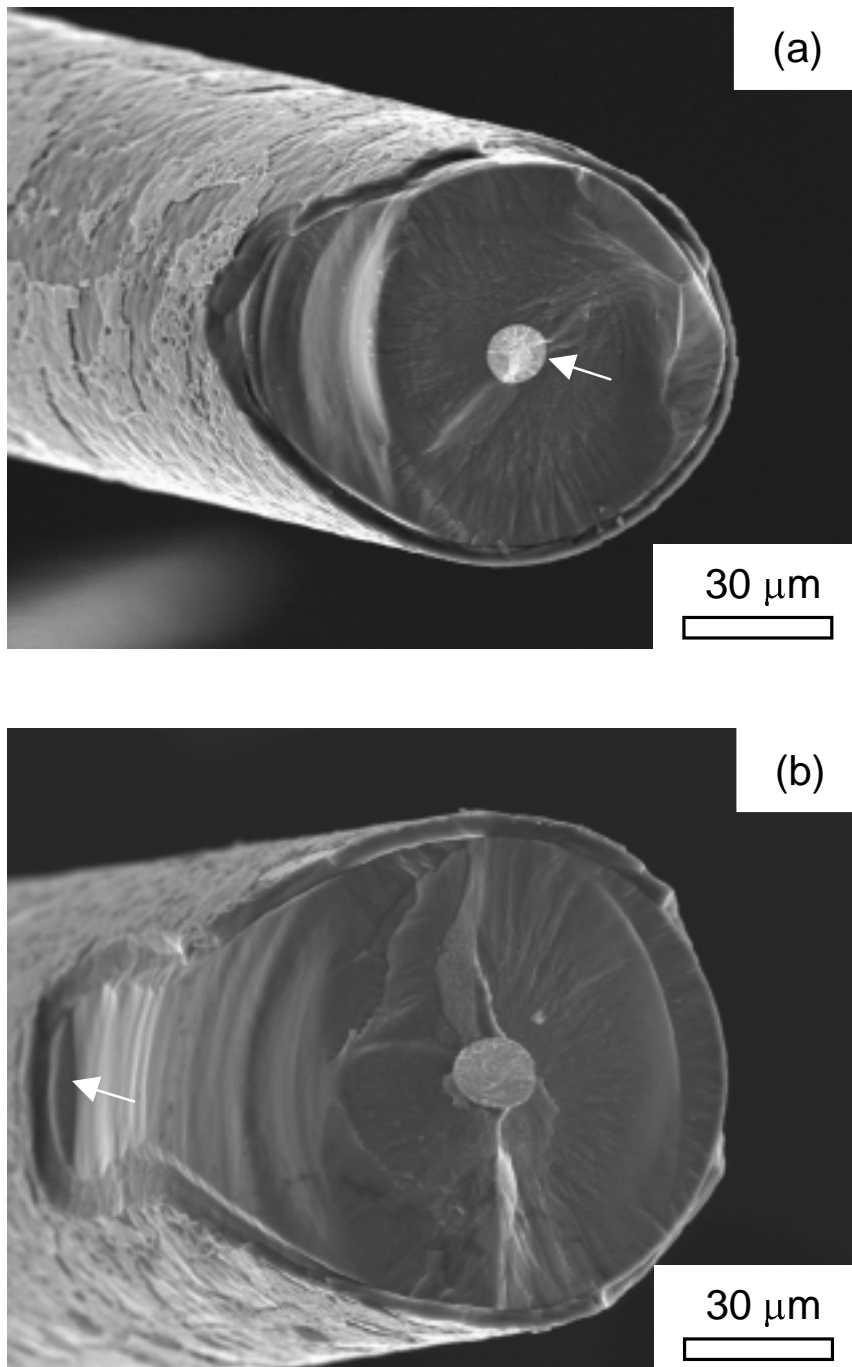


Figure 5: Fracture surfaces of as-extracted fibres (a) High strength fibre (3.13 GPa.) (b) Low strength fibre (2.51 GPa.). The critical flaws responsible for the fibre fracture are shown by the arrows.

Acknowledgements

The authors wish to express their gratitude to Drs. J. Y. Pastor and P. Poza for their help in the mechanical tests and in the fractographic analyses. This financial support from CICYT and the European Union through grant 2FD97-89-C02-02 is also gratefully acknowledged.

REFERENCES

1. Cheng, T. T., Jones, I. P., Shatwell, R. A., and Doorbar, P. (1999) *Mater. Sci. Engng.* **A260**, 139.
2. Chawla, K. K. (1998) *Fibrous Materials*. Cambridge Solid State Science Series. Cambridge.
3. Shatwell, R. A. (1994) *Mater. Sci. Techno.* **10**, 552.
4. Hurst, J. B., Hong, W. S., Gambone, M. L., and Porter, J. R. (1998) In: *Inter. Gas Turbine & Aeroengine*

Congress & Exhibition. Paper 98-GT-567. American Society Mechanical Engineers, New York.

5. Ocaña, I., Martín Meizoso, A., Gil Sevillano, J., Fuentes Pérez, M. (1997) *Anal. Mec. Frac.* **14**, 288
6. Baker, A. M., Grant, P. S., and Jenkins, M. L. (1999) *J. of Microscopy* **196**, 162.
7. Dyos, K., and Shatwell, R. A. (1999) *J. of Microscopy* **196**, 175.
8. Heath, S. P. (1990) Report 137 724. BP Metal Composites, Middlesex.